



# FTIR-ATR characterization of free *Rhizomucor meihei* lipase (RML), Lipozyme RM IM and chitosan-immobilized RML

Sebastián Enrique Collins<sup>a,\*</sup>, Verónica Lassalle<sup>b</sup>, María Luján Ferreira<sup>c</sup>

<sup>a</sup> INTEC, UNL-CONICET, Güemes 3450, Santa Fe 3000, Argentina

<sup>b</sup> INQUISUR, UNS, Avenida Alem 1253, 8000 Bahía Blanca, Argentina

<sup>c</sup> PLAPIQUI-UNS-CONICET, Camino La Carrindanga Km 7, CC 717, 8000 Bahía Blanca, Argentina

## ARTICLE INFO

### Article history:

Received 15 April 2011

Received in revised form 3 June 2011

Accepted 7 June 2011

Available online 17 June 2011

### Keywords:

Biocatalysis

Lipase from *Rhizomucor meihei*

Infrared spectroscopy

FTIR-ATR

## ABSTRACT

The synthesis and characterization of biocatalysts based on lipase from *Rhizomucor miehei* (RML) immobilized on chitosan-based supports were investigated. The enzyme was immobilized on chitosan following two strategies: (i) physical adsorption; and (ii) covalent bonding using glutaraldehyde. The content of enzyme bound in the supports, as precipitable protein, was analyzed using UV/visible methods. FTIR-ATR spectroscopy was employed to characterize the prepared biocatalysts, as well the native enzyme and a commercial biocatalyst Lipozyme RM IM, used as reference materials. Analysis of the amide I' signal allowed to follow the changes in the secondary structure of the enzyme after binding to the support and its thermal stability. The hydrolysis of ethyl stearate monitored in situ by FTIR-ATR was used as a test reaction. Results showed that RML was bound to Chit and Glut-Chit with minor changes in its secondary structure, thermal stability and enzymatic activity in a selected reaction test.

© 2011 Elsevier B.V. All rights reserved.

## 1. Introduction

Lipases (triacylglycerol hydrolases) are special enzymes that hydrolyze triacylglycerol at the lipid/water interface. These enzymes have technological importance due to their increasing utility in food industry processes [1] and pharmaceuticals, in e.g. enantio-selective purification [1–3]. However, the use of commercial lipases in its native free-form is limited by the difficulty of their recovery. Thus, lipases must be anchored on a suitable support, insoluble in the reaction medium, to enable their re-use and to be applicable to the industrial scale. Nevertheless, the process of immobilization may induce alterations in the conformation of the enzyme producing a loss of activity [4], which has to be investigated in order to design better biocatalysts.

Among several supports employed for the immobilization of enzymes, chitosan (Chit) has shown suitable characteristics for this purpose [5–8]. Chit is a polysaccharide, made by monomers of D-glucosamine, which is obtained from the shells of mollusks. It is hydrophilic but insoluble in water and other polar/non-polar solvents. Also, it has interesting biological and chemical properties: it is biodegradable, biofuel-compatible, bioactive, poly-cationic in aqueous solution, and may be chemically modified in a variety of ways [9,10]. The morphology of Chit particles makes it a suitable

material for enzyme immobilization [8]. Thus, some of us reported on the immobilization of *Candida antarctica* lipase B (CALB), *Candida rugosa* lipase (CRL) and *Pseudomonas fluorescens* lipase (PFL) in hydrophobic supports (such as polypropylene) and a hydrophilic biopolymer (chitosan) to generate bioactive and selective catalysts for the solvent-free synthesis of ethyl oleate [11] and, more recently, the enantiomeric resolution of R/S ethyl esters of ibuprofen [3].

Usually, enzymes are immobilized onto supports by adsorption and covalent bonding. Adsorption is a complex process where Van der Waals forces, electrostatic interaction between charged groups on the surface of the enzyme and substrate and hydrogen-bonding are involved [12]. In the case of covalent coupling, a bond is formed between the functionalized support and one or more functional groups of the enzyme. Glutaraldehyde (Glut) is one of the most common compounds used to functionalize chitosan. Particularly, Glut has been employed to modify Chit, due to formation of an imine (C=N) bond between NH<sub>2</sub> groups of Chit and aldehyde groups of Glut, which leave the other aldehyde group to react with the amine groups of side chains of amino acids of the enzyme, such as lysine [13].

Immobilization of enzymes can change their secondary structure modifying its activity. Conformational study of enzyme–protein structures can be made by spectroscopic techniques such as circular dichroism (CD) and infrared (IR), both in its free-state as well as in its immobilized form [14,15]. IR spectroscopy has the advantage of being a technique of narrow

\* Corresponding author.

E-mail address: [scollins@santafe-conicet.gov.ar](mailto:scollins@santafe-conicet.gov.ar) (S.E. Collins).

bandwidth, thus a good correlation between the signals recorded in the zone of amide I ( $1700\text{--}1600\text{ cm}^{-1}$ ) and the secondary structure of proteins have been established [15–17]. In particular, IR spectroscopy in attenuated total reflectance mode (ATR) allows the in situ study of enzymes or proteins in liquid and/or solid phase.

This work presents the results of preparation and characterization by ATR-IR of *Rhizomucor miehei* lipase (RML) immobilized on bare and glutaraldehyde-functionalized chitosan. The amount of immobilized enzyme is carefully quantified by means of a simple and accurate UV–vis method. After isotopic exchange with  $\text{D}_2\text{O}$ , the analysis of the amide I' band brings important information about changes suffered by RML anchored in the support, which is relevant to correlate with enzymatic activity at selected reactions and selected conditions. Additionally, the thermal-induced modifications in the secondary structure are investigated in situ, as well the enzymatic activity obtained in a simple and fast method, which are important to know about the efficiency and activity of immobilized forms. With these goals, the manuscript presents how this information can be obtained with ATR mode about the RML conformation, thermal stability and enzymatic activity in free vs immobilized forms. This kind of approach may avoid more expensive and time-consuming activity measurements, even when the catalytic results presented here are qualitative. However, it is clear that the immobilized RML on bare chitosan and on glutaraldehyde modified chitosan retains their activity. This fast measurement of the hydrolytic activity may be useful to select some group of immobilized lipases vs others for more sophisticated reaction tests.

## 2. Experimental

### 2.1. Biocatalysts

Pure lipase from *Rhizomucor miehei* (RML) – in aqueous solution – and Lipozyme RM IM (*Rhizomucor miehei* lipase immobilized on a macroporous ion exchange resin) were kindly provided by Novozymes (Brasil). An aqueous solution of 25% wt/wt Glut (Fluka) was used. Biocatalysts based on immobilized RML onto chitosan were prepared in our laboratory. Chitosan from Chitoclear, *Pandalus borealis* (Primex, Iceland) with a deacetylation degree of 92% (Colloidal Titration) and a viscosity of 7 cP (1% chitosan solution) was employed as support. Two strategies were chosen to prepare these samples: (i) a physical adsorption and (ii) a covalent bonding to the support using Glut.

0.5 ml of commercial solution of RML (5000 U/ml-equivalent to near 100 mg of precipitable protein (PP) using ammonium sulfate) and 200 mg of chitosan were dispersed in 5 ml of bi-distilled water in a vial of 10 ml, and stirred vigorously for 4 h at room temperature. This procedure generated the biocatalyst RML/Chit. After immobilization, the resulting biocatalyst was filtered, washed three times with distilled water and dried to constant weight at room temperature. The washing solutions were analyzed to measure the amount of desorbed protein at the washing steps. Due to the complexity of commercial lipase solution, the biocatalysts will be characterized in terms of the PP content, as a measurement of the RML content.

The goal of the manuscript was to use the chitosan as received. We have found that at long immobilization times of the enzyme or protein, chitosan dissolves partially. This information, however, was taken into account in the determination of the amount of PP immobilized on chitosan.

Glut–Chit support was prepared by mixing a Glut solution with a dispersion of chitosan in bi-distilled water (37.5 mg Glut/1 g Chit/25 ml  $\text{H}_2\text{O}$ ). The reaction was carried out under vigorous magnetic stirring at  $45^\circ\text{C}$  (2 h). Then, a similar methodology was employed to bind the RML to the Glut–Chit support to generate the

RML/Glut–Chit biocatalyst. Also a similar purification procedure through 3 washing steps was applied.

About the strength of remaining RML on chitosan, it is clear from the washing steps that only the first washing desorbed the highest amount of RML (near 80% of the full amount of the total desorbed RML) being the other two washing steps of lower importance. The remaining enzyme is strongly bonded to the support, and active. The tests done on the ATR mode demonstrated no desorption of the lipase in the measurement time (see below).

The protein content in each support was determined through a mass balance from the initial amount of protein from the commercial RML, the mass lost during washing procedures and the non-immobilized protein remained in the supernatant. The PP contents were measured through UV/visible spectroscopy using the absorbance at 280 nm technique [17]. The data were reported as percentage of PP relative to the total biocatalyst mass; and calculated as follows:

$$\%PP = \frac{\text{mg PP}_{\text{initial}} - \text{mg PP}_{\text{in supernatant}} - \text{mg PP}_{\text{in washings}}}{\text{mg}_{\text{recovered biocatalyst}}} \times 100$$

where  $\text{PP}_{\text{initial}}$  stands for the initial amount of protein from the commercial RML;  $\text{PP}_{\text{in supernatant}}$  stands for the amount of protein remained during the immobilization procedure; and  $\text{PP}_{\text{in washings}}$  stands for the amount of protein desorbed during the washings.

### 2.2. In-situ infrared spectroscopy

Infrared spectra of biocatalysts based on RML were acquired in situ as a function of temperature and time using attenuated total reflection (ATR) cell. To achieve an accurate analysis of secondary structure based on amide I mode, all samples were studied after being subjected to an isotopic exchange with  $\text{D}_2\text{O}$  as described below. This procedure allows the observation of IR signals in the amide I region ( $1700\text{--}1600\text{ cm}^{-1}$ ) without the interference of the  $\delta(\text{OH})$ , the water signal at  $1640\text{ cm}^{-1}$  [15,16].

RML, from its commercial concentrated solution, was deposited as a homogeneous film on the ATR crystal after evaporation of the aqueous solvent. Then, 200  $\mu\text{l}$  of  $\text{D}_2\text{O}$  ( $\text{D} > 99.7\%$ ) was added to the film and the cell was closed and incubated at room temperature overnight to allow isotopic exchange occurs. The cell was purged with dry  $\text{N}_2$  (99.999%) for 3 h to remove excess of  $\text{D}_2\text{O}$  and remaining traces of  $\text{H}_2\text{O}$ . Next, 200  $\mu\text{l}$  of  $\text{D}_2\text{O}$  was added to the cell, again. This procedure ensures complete isotopic exchange of the enzyme.

In the case of solid biocatalysts about 1 mg was dispersed in 500  $\mu\text{l}$  of  $\text{D}_2\text{O}$  by vigorous stirring for 10 min. The previous slurry was dropped on one side of the ATR crystal using a micropipette. Then, the catalyst layer was dried in situ by flowing  $\text{N}_2$  (99.999%) at r.t (3 h). The solvent evaporated leaving the catalyst particles homogeneously distributed onto the crystal surface.

The cell was mounted onto an ATR attachment (Pike Technologies) inside the sample compartment of the FTIR spectrometer (Thermo-Electron, Nicolet 8700 with a cryogenic MCT detector). The bench of the spectrometer was continuously purged with dried air (Parker Balston FTIR purge gas generator) to eliminate  $\text{CO}_2$  and water vapor contributions to the spectra. Time-resolved ATR-FTIR spectra were recorded in kinetic and rapid-scan mode at a resolution of 0.5 and  $4\text{ cm}^{-1}$ . The cell temperature was controlled within  $\pm 0.5^\circ\text{C}$  with a thermostatic water bath (Julabo) connected to the heating jacket of the cell.

### 2.3. Catalytic test

Hydrolysis of ethyl stearate was studied for free and immobilized RML, monitoring the progress of the reaction using time-resolved in situ ATR. A solution of 7 mg/ml of ethyl stearate (98%, Sigma) in iso-octane was mixed with a determined amount

**Table 1**  
Precipitated protein – PP – from RML in the biocatalysts.

Support <sup>a</sup>	RML in supernatant (mg)	RML in washings (mg)	Mass of recovered biocatalyst (mg) <sup>c</sup>	%RML in biocatalyst
Chit	72	10	177.6	10.1
Chit–Glut	<sup>b</sup>	<sup>b</sup>	167.5	<sup>b</sup>

<sup>a</sup> Initial amounts: 200 mg support; near 100 mg PP from commercial RML.

<sup>b</sup> The determination was not possible. See the discussion in the text.

<sup>c</sup> The differences in mass balance could be attributed to the partial dissolution of Chit (see the discussion in the text.)

of biocatalyst (5–8 mg) and a molar ratio of 2:1 water:ester. The ATR cell was filled with this dispersion. Subsequently, the cell was closed and heated at 36 °C. The hydrolysis yield was measured by the decrease of the carbonyl ester absorption peak ( $1745\text{ cm}^{-1}$ ) over time, and quantified by integrating this peak in the interval  $1760\text{--}1700\text{ cm}^{-1}$ . Meanwhile, the stearate ester conversion was followed through the increase of the characteristic signal of stearic acid at  $1700\text{ cm}^{-1}$ . In an additional experiment, the linear response of the bands at  $1745\text{ cm}^{-1}$  for the ester and at  $1700\text{ cm}^{-1}$  for the acid was corroborated by measuring the integrated area for solutions with different concentrations in isooctane.

### 3. Results and discussion

#### 3.1. Preparation of biocatalysts

The protocol employed in the biocatalysts preparation is quite simple and non-time-consuming. Reproducible results were obtained using this method in a series of preparations.

The amount of protein immobilized onto the chitosan-based supports was carefully determined. However, some experimental difficulties were found during the PP quantification, which are worth to mention. Two different methods were employed to measure the PP content in the immobilized biocatalysts: (i) the analysis of the PP when possible through a direct UV/visible method, and (ii) the comparison of the enzymatic activities using RML–Chit or RML as reference (results not shown). Method (ii) will be discussed later.

Using the UV/visible quantification procedure, results of the amount of PP adsorbed on Chit were more accurate than with the other methods (using the enzymatic activity). The UV/visible simple method used here takes into account the protein aggregation, the use of the same protein to quantify as standard and the application of bi-distilled water as the adsorption and measurement media. These strategies were implemented to avoid quantification mistakes and were based on previous work [18].

Additionally, the contribution of the solubilization of chitosan during the RML immobilization was evaluated as an additional error source in the quantification of PP by UV/visible measurements. Chitosan was incubated in bi-distilled water following the immobilization protocol. UV/visible spectra were recorded at initial and final selected time. Chit contributes in the UV/visible region in this experiment. The solubilization of low molecular weight Chit upon interaction with the RML cannot be ruled out, especially with the problems in the PP quantification found during the immobilization of RML on Glut–Chit. The contribution of the dissolution of pure Chit was considered to calculate the percentage of RML adsorbed on Chit. The dissolution of pure Chit under the same experimental conditions than in RML immobilization was about 10.1%, wt/wt. A fraction of Chit of low molecular weight was dissolved during the RML immobilization and lost during the washing steps. This fraction was found as large as the 20% of the initial Chit based on the mass balance considering the initial amounts of Chit and RML and the final mass of biocatalyst recovered (see Table 1). The same situation was also observed in the case of RML/Glut–Chit.

The protein quantification by UV/visible methods is a tedious task to obtain reproducible results. The data from the PP quantifi-

cation are listed in Table 1. The mass of protein lost during the washing steps could be ascribed to protein weakly adsorbed on the Chit surface, which is removed upon contact with bi-distilled water. This step is very important to avoid leaching of weakly adsorbed protein in the reaction media.

In the case of Glut–Chit support, a reliable result of the amount of adsorbed PP from RML was not obtained. Confusing results were found trying to quantify protein by UV/visible spectroscopy. Fig. 1 shows the UV/visible spectra of the sample obtained from the RML immobilization supernatant at initial and final stages. The baseline is missing, and also the band at 254 nm, typical of RML. The spectra show a broad band from 290 nm up to 500 nm, a zone when the diluted RML does not show any bands. This could be attributed to several possible causes: (i) a very fast adsorption of the enzyme on the support, (ii) the interference of the dissolved Chit and/or Glut desorbed – from weakly adsorbed Glut – in the region of UV/visible absorption of the PP, from the commercial RML, (iii) a fast dissolution of low molecular weight Chit upon strong magnetic stirring, with contribution in the 200–500 nm zone, and (iv) a colloidal dispersion of low molecular weight Chit or Glut–Chit, introducing a dispersive effect on the spectra, increasing absorbance of the baseline. In order to check some possible interferences of the support in the quantification of PP, the Glut–Chit was incubated in bi-distilled water in absence of RML, at the experimental conditions of the RML immobilization. The shape of the spectrum is considerable different than the one observed in the Fig. 2, especially in the 240–300 nm range. A distortion of the baseline is found in the region where the typical Glut band is located (293 nm). A signal at 235 nm is also observable in agreement with that observed in the Fig. 1. Therefore this band could be assigned to the fraction of soluble Chit or a Chit derivative arising from its reaction with Glut. It is known that soluble Chit exhibits a band near 190–214 nm (results not shown and [19]). In this case the difference between the original amounts (mg) of the raw materials and the final mass of recovered biocatalysts supports the hypothesis of the Chit dissolution. In agreement with

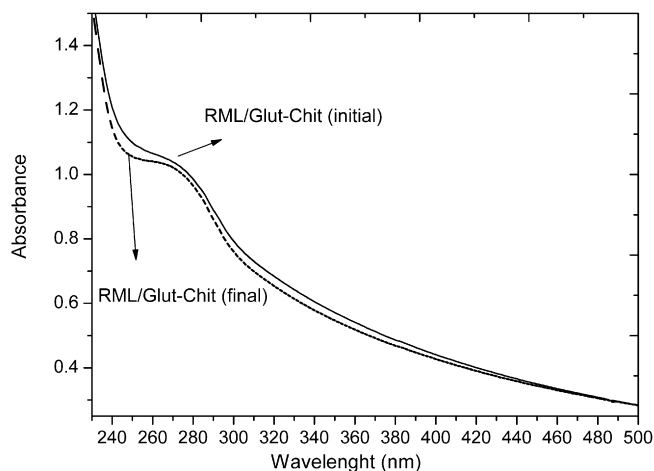


**Fig. 1.** UV/visible spectra of the sample obtained from the RML immobilization supernatant at initial and final stages.

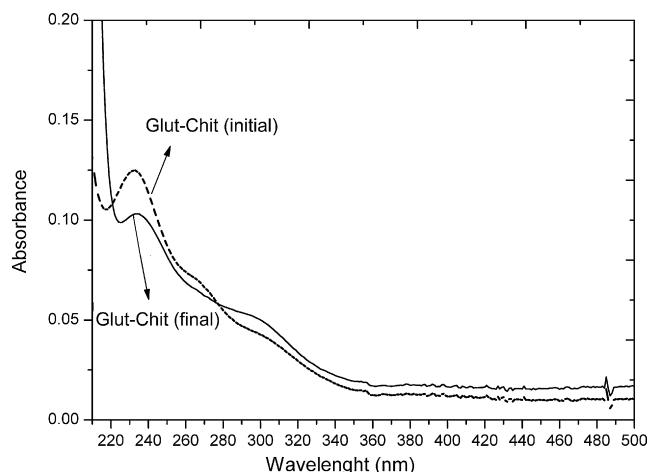


**Fig. 2.** UV/visible spectra of the sample obtained from Glut-Chit support at initial and final stages.

the analysis exposed above, we suggest that any UV/visible based-method, even those with reaction such as Bradford, Lowry or the Bichinonic Acid (BCA) ones, will cause erroneous protein quantification data regarding to the immobilization of RML in this kind of supports. Therefore alternative techniques are currently under analysis to quantify protein content in this case.

### 3.2. Spectral/conformational analysis

Fig. 3 shows the infrared spectra at room temperature of pure RML before and after the complete isotopic exchange with  $D_2O$ . Amide I band, corresponding to  $\nu(CO)$  carbonyl stretching mode of the peptide, is present in the region of  $1700$ – $1600\text{ cm}^{-1}$  [15–17]. This band consists of a group of overlapped signals, which contain information on secondary protein structure of the enzyme.

Bands centered at around  $1547\text{ cm}^{-1}$  are assignable to the amide II band, which is a out-of-phase combination mode of the NH in plane bend and the CN stretching vibration with smaller contributions from the CO in plane bend and the CC and NC stretching vibrations [15]. Additionally, the peak at  $1590\text{ cm}^{-1}$  can be assigned to the asymmetric stretching mode of carboxylic groups,  $\nu(COO)$ , of aspartic acid (Asp A.) and/or glutamic acid (Glu A.) in side chains [15].

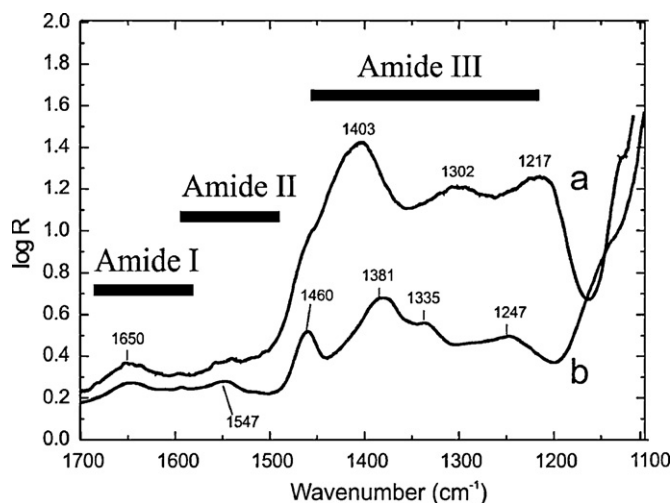


**Fig. 3.** Infrared spectra of pure RML before (a) and after (b) the isotopic exchange with  $D_2O$ .

**Table 2**

Assignment for amide I' band position to secondary structure [15–17].

Secondary structure	Band position of amide I' ( $D_2O$ ) $\text{cm}^{-1}$	
	Average	Extremes
$\alpha$ -Helix	1652	1642–1660
$\beta$ -Sheet	1630	1615–1638
	1679	1672–1694
Unfold/aggregated	1612	1605–1625
Disordered/random	1645	1639–1654

Finally, a set of bands can be distinguished in the region of  $1400$ – $1200\text{ cm}^{-1}$  due to amide III mode. This mode is assigned to the in-phase combination of the NH deformation vibration with CN, with a minor contribution of CO and CC stretching. These polypeptide bands are complex and do not allow a direct correlation with the protein structure [15–17,20]. Amide III peaks are better resolved after deuteration due to loss of coupling with the  $\delta(NH)$  vibration. This information was used to evaluate the degree of deuteration achieved.

The secondary structure, after the complete exchange with  $D_2O$ , was studied using the amide I' band. The interference of the strong band at  $1630\text{ cm}^{-1}$  of  $H_2O$ , which is impossible to suppress in the supported samples, was avoided.

Table 2 summarizes the commonly reported assignments for signals in the amide I' region. Due to the high degree of overlap in the amide I' band, an analysis of reduced bandwidth was first performed [16]. This analysis was accomplished using the second derivative of each spectrum in the region of  $1700$ – $1600\text{ cm}^{-1}$ , and by Fourier Self-Deconvolution (FSD) – not shown – to identify the position of each band in this region. Fig. 4A shows, as an example, the second derivative spectrum in the region of amide I' for pure RML sample. It is possible to identify up to six components in the

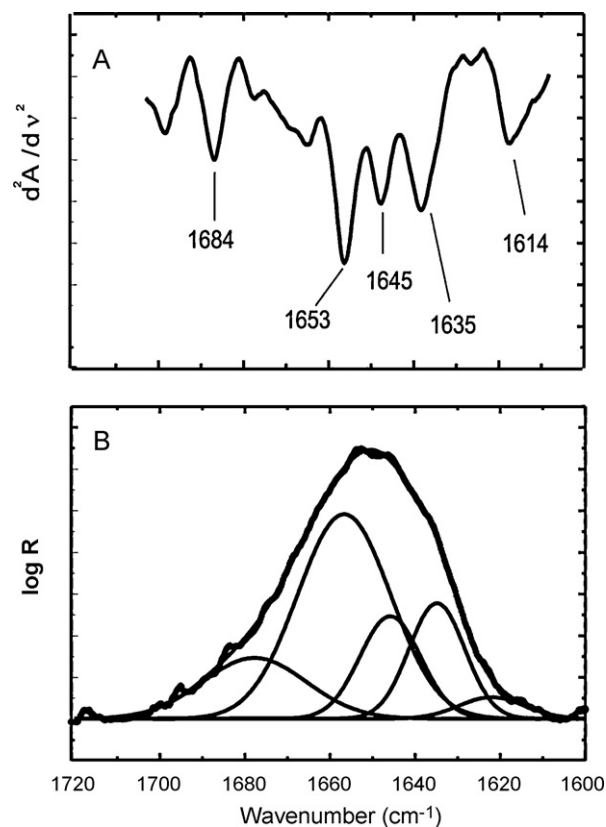


**Fig. 4.** A second derivative spectrum in the region of Amide I' for pure RML (A), and deconvolution of the overlapped bands (B).



**Table 3**  
Secondary structure in each biocatalyst.

Biocatalyst	Secondary structure		Glu A.–Asp A./amide I'
	$\alpha$ -Helix	$\beta$ -Sheet	
RML	48	32	0.2
Lipozyme	30	46.5	0.2
RML/Chit	32	48	0.1
RML/Glut–Chit	15	54.5	–
DRX-RML <sup>a</sup>	45	41	–

<sup>a</sup> Ref. [22].

spectrum. A Gaussian-sum function was used to fit the overlapped bands, measuring peak position and areas. The best fit was used to estimate the percentage contribution of each band to the spectrum of amide I' as shown in Fig. 4B.

$\alpha$ -Helices show a strong and characteristic absorption band centered at  $1653\text{ cm}^{-1}$ . Additionally, it is also possible to identify a band at  $1645\text{ cm}^{-1}$ , which can be assigned to random structures [15–17,20].  $\beta$ -Sheets have two signals at  $1635$  (intense) and  $1683\text{ cm}^{-1}$  (weak) [15]. The splitting of the amide I mode in  $\beta$ -sheets structures is a consequence of differences in hydrogen-bridged bonds and the dipole transition coupling. The band at  $1683\text{ cm}^{-1}$  may also contain overlapping contributions (i.e. that could not be resolved in our spectra) due to turn structures [15]. A low intensity peak at  $1614\text{ cm}^{-1}$  can be assigned (see below) to unfold or aggregated  $\beta$ -sheet structures [21].

Table 3 presents the percentage of secondary structures for pure RML estimated from the ATR infrared spectrum. This result is in reasonable agreement with the reported secondary structure of RML from the analysis of its crystal structure by X-ray diffraction [22]. Likewise, Goormaghtigh et al. [23,24] published, using a 50-protein database, that the secondary structure prediction by infrared analysis has a relative overall error below 10%.

The same approach was employed to analyze the secondary structure in the supported biocatalysts. Nevertheless, as discussed below, signals coming from the support complicate the analysis of the amide I' region. The spectra for each support and biocatalyst are reported in Fig. 5. Table 3 presents the results of the deconvolution of the spectra obtained for each sample.

Fig. 5 shows in comparative form the spectra in the region of  $1750\text{--}1500\text{ cm}^{-1}$  of the investigated samples: pure RML, Lipozyme RM IM, RML/Chit, RML/Glut–Chit, along with Chit and Glut–Chit. In

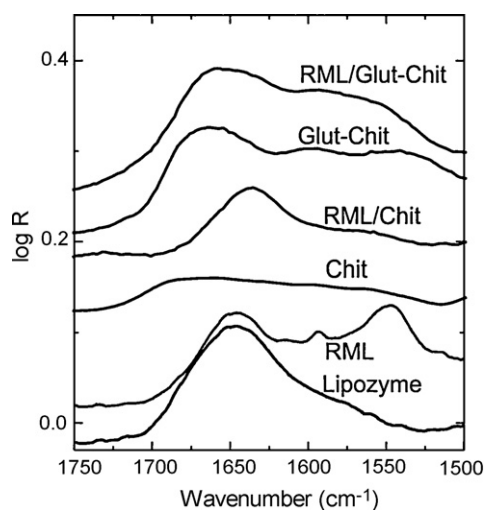


**Fig. 5.** ATR-FTIR spectra in the region of  $1750\text{--}1500\text{ cm}^{-1}$  of the investigated samples: pure RML, Lipozyme RM IM, RML/Chit, RML/Glut–Chit, along with Chit and Glut–Chit bare supports.

general, it is clear that there are differences in the distribution of signals in the  $1700\text{--}1600\text{ cm}^{-1}$  region.

The infrared analysis of protein secondary structure in the Lipozyme RM IM sample is further complicated by the presence of an intense peak centered at  $1636\text{ cm}^{-1}$ . This signal corresponds partially to the support polystyrene-divinyl-benzene resin [25]. After spectral deconvolution signals contributions were identified due to  $\beta$ -sheets (46%) and  $\alpha$ -helices (30%), see Table 3. It is worth to note here that the relative error in this analysis may increase as a consequence of the support signal in this region. Nevertheless, the secondary structure estimated from the infrared results allows concluding that protein conformation has been mostly preserved, which is in good agreement with the results of catalytic activity of this material in selected reactions [26,27].

The spectrum of bare chitosan support, showed in Fig. 5, presents a broad band in the  $1700\text{--}1500$  region due to  $\delta(\text{OH})$  and  $\delta(\text{NH}_2)$  modes of the polyamine-saccharides [28–30]. The presence of the amide I' band can be clearly discerned by comparing the spectra of RML/Chit with the one of pure chitosan in Fig. 5. In order to estimate the protein secondary structure in the RML/Chit biocatalyst, it was necessary to subtract the contribution of chitosan signals to the spectra. Additionally, the band shape in RML/Chit is different from that of pure RML, which indicates that some changes have occurred in the conformation of the enzyme after adsorption to the support. As seen in Table 3, the conformational changes observed in the enzyme indicate that part of the  $\alpha$ -helix structure have been lost, probably giving rise  $\beta$ -sheet and/or self-aggregates [20].

It is also possible to estimate the relationship between the bands between  $1560$  and  $1600\text{ cm}^{-1}$  assigned to  $\nu(\text{COO}^-)$  of deprotonated amino acids (Glu A. and/or Asp A.) in side chains as compared to the total area of amide I' ( $1600\text{--}1700\text{ cm}^{-1}$ ), as shown in Table 3. Although the protonation of side groups depends on the pH of the solution of immobilization, it has been reported that the enzyme retains, as a “memory effect”, the pH of the solution of immobilization [13]. It can be noted that the relative amount of deprotonated amino acid Glu, and/or Asp in side chains in the RML/Chit catalyst is lower than in the free RML (Table 3). This result could indicate that the enzyme links to the support through the negatively charged side chains that may form hydrogen bonds and/or by protonation via  $\text{NH}_3^+$  groups of chitosan at the immobilization pH (5.8).

As it has been mentioned, chitosan has a hydrophilic nature, while RML has many non-polar amino acids in its structure. Chitosan presents a distribution of  $\text{NH}_2/\text{NH}_3^+$  groups which depends on the solution pH. The  $\text{NH}_2/\text{NH}_3^+$  fraction approaches to 0.5 at a pH near to 6 [31]. Thus, it is expected that the interaction between RML/Chit be a combination of: (i) ionic, through charged amino acids, e.g. Asp A. and Glu A. of the protein with  $\text{NH}_3^+$  groups of chitosan, and (ii) via Van der Waals forces and hydrogen bonding involving  $\text{NH}_2/\text{OH}$  groups of chitosan.

The infrared spectra of Glut–Chit and bare Chit are compared in Fig. 6 in the  $2000\text{--}900\text{ cm}^{-1}$  region. As shown in the spectra, a set of new bands appeared in the modified Chit sample after the binding of glutaraldehyde: (i) a weak shoulder at  $1710\text{ cm}^{-1}$ , assigned to  $\nu(\text{C=O})$  mode of remaining aldehyde groups of Glut; (ii) a group of bands at  $1660\text{ cm}^{-1}$  (increased as compared with bare support) and  $1598\text{ cm}^{-1}$ , assigned to the imine bond  $\nu(\text{N=C})$  produced after the reaction of aldehyde with amine groups, which revealed the Schiff's base formation [28,32], and (iii) a signal observed at  $1548\text{ cm}^{-1}$ , better resolved in the spectrum of Glut–Chit, attributed to the formation of an ethylenic double bond in the chitosan–glutaraldehyde interaction in crosslinked structures [31]. Similar results have been reported by Monteiro and Airoidi [28] in studies of the functionalization of chitosan with glutaraldehyde by FTIR and Raman spectroscopies.

After comparing the ATR spectra of functionalized support Glut–Chit with the biocatalyst RML/Glut–Chit, a shoulder emerged

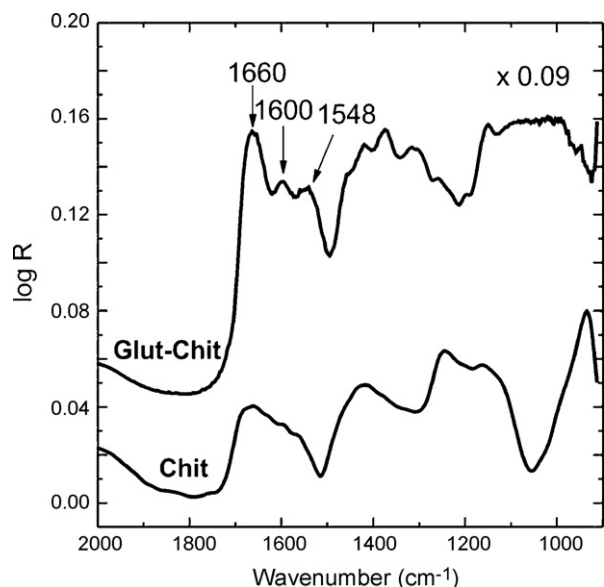


Fig. 6. Infrared spectra of Glut–Chit and Chit in the 2000–900  $\text{cm}^{-1}$  region.

at higher frequencies from the main band centered at  $1684\text{ cm}^{-1}$ . This band was not present in the spectrum of RML/Glut–Chit. At the same time, there is a (slight) increase in signal intensity of the imine band at  $1598\text{ cm}^{-1}$ . This result indicates that indeed the residual aldehyde group in the Glut reacted with  $\text{NH}_2$  residues present in the lipase to form a covalent protein–substrate link.

Fig. 7 shows schematically the enzyme–support interactions identified for the biocatalyst RML/Glut–Chit. It has been proposed that the reaction of Glut with lipases takes place through mainly the reaction of lateral groups of lysine residues from proteins

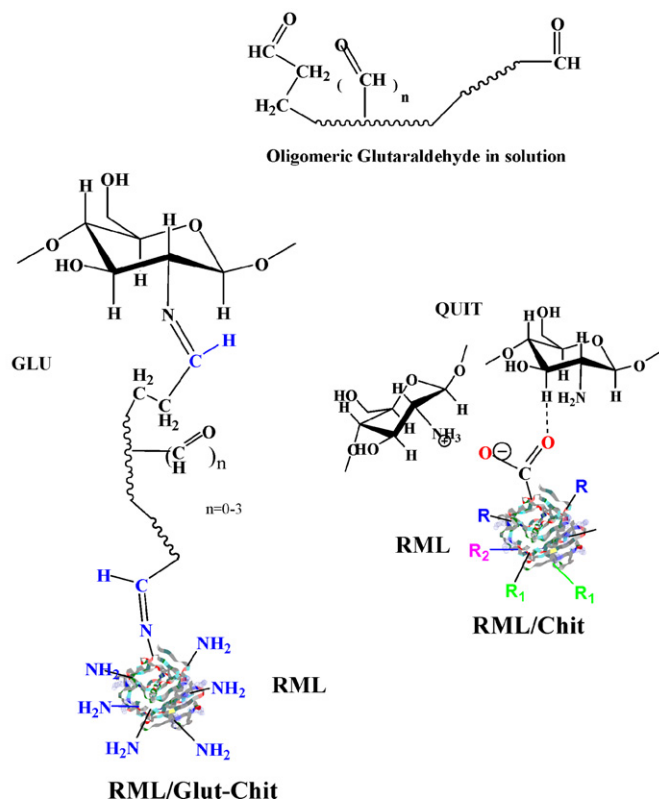


Fig. 7. Scheme of the enzyme–support interactions identified for the RML/Glut–Chit and RML/Chit biocatalysts. RML imagen from [37].

[33]. RML has seven lysine groups per molecule (3tgi-Protein Data Bank). Therefore it is expected a higher rigidity and stability in RML/Glut–Chit biocatalyst vs RML–Chit. Additionally, given the diversity of exposed amino acid side groups, it cannot be ruled out that other polar side groups than lysine were involved in the immobilization. Besides, the 25% Glut solution is not present as monomer, but it contains a wide distribution of products by aldolic condensation [34,35]. Glutaraldehyde in aqueous solution suffers several types of reactions, such as aldol condensation, hydration, hydration–polymerization and oxidation [36]. Therefore, the RML/Glut interaction may be rather complex.

The main signals that conforms the band between 1700 and  $1600\text{ cm}^{-1}$  in the spectrum of RML/Glut–Chit were deconvoluted using the same criteria described above. However, the uncertainty introduced by the consumption of remnant aldehyde and the increase of signals due to the new imine bonds as compared with the Glut–Chit support, hampers a detailed analysis of secondary structure of the enzyme in this material.

The combination of UV/visible and ATR-FTIR results allows to draw several conclusions: (i) RML adsorbs from very strongly to weakly on bare Chit with changes in the ATR-FTIR signals assignable to some minor modifications in its secondary structure; (ii) there is a partial dissolution of Chit or complexes Glut–Chit and also  $\text{RML} \times \text{Chit}$  and  $\text{RML} \times \text{Glut} \times \text{Chit}$  during the immobilization step, (iii) RML reacts with Glut adsorbed or reacted on Chit and it may produce soluble species that interfere with the UV/visible simple methods; (iv) treatment of the supports Chit or Glut–Chit at the same experimental conditions of RML immobilization are not useful as “blanks” due to the impact of the RML in the solubilization of Chit or Glut–Chit; (v) washing steps after immobilization are crucial to avoid the presence of weakly adsorbed RML in RML/Chit; and (vi) Glut in RML/Glut–Chit interferes with the analysis of the changes in the secondary structure after covalent binding of RML.

### 3.3. Thermal stability

The immobilization process onto a solid support can also influence the thermal stability of the enzyme. The IR spectra of a pure RML film are shown in Fig. 8 in the amide I' region, after 90 min at 30, 60, 70 and  $90^\circ\text{C}$ . From  $70^\circ\text{C}$ , an infrared peak shows up at  $1620\text{ cm}^{-1}$ , together with a broader band centered at  $1678\text{ cm}^{-1}$ . At the same time, there is a decrease in the band at  $1653\text{ cm}^{-1}$ , previously assigned to  $\alpha$ -helices. Likewise, significant changes in

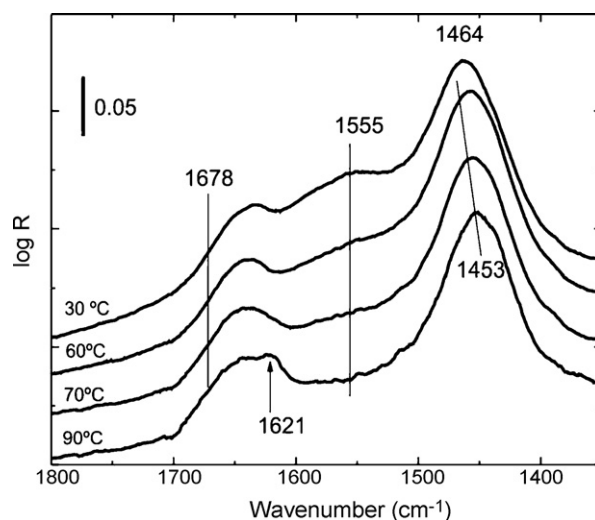


Fig. 8. ATR-FTIR spectra of pure RML sample in the amide I' region after 90 min at 30, 50, 70 and  $90^\circ\text{C}$ .

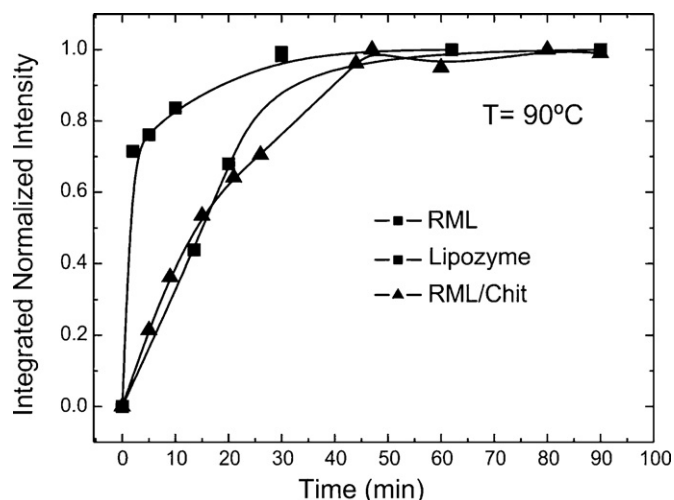


Fig. 9. Temporal evolution of the normalized signal at  $1620\text{ cm}^{-1}$  for RML, Lipozyme and RML/Chit at  $90^\circ\text{C}$ .

the area of amide II' and III' (not shown) were also observed in the spectra, which are also correlated with structural changes affecting the protein.

A distinctive band at  $1620\text{--}1615\text{ cm}^{-1}$  accompanied by a signal of lower intensity at  $1678\text{ cm}^{-1}$ , is attributed to aggregated  $\beta$ -sheet structures formed by polypeptide chains unfolded by temperature.  $\beta$ -Sheets interact with each other forming aggregates linked by strong hydrogen bonds. From  $70^\circ\text{C}$  onwards, the structure of the protein suffers a conformational change, where  $\alpha$ -helix unfold to form  $\beta$ -sheet aggregates through hydrogen bridge bonds [21]. Thus, the IR signal at  $1620\text{ cm}^{-1}$  can be used as a good measure of the degree of unfolding/thermal denaturation of proteins and, therefore, the thermal stability of the lipase.

After heating the sample at  $90^\circ\text{C}$  for 90 min, the ATR cell was cooled to room temperature. The spectra collected showed that the signals due to aggregate/self-assembled structures were similar to those observed at  $90^\circ\text{C}$ . Thus, the changes in the secondary structure of RML were irreversible. In order to compare the thermal stability of the set of biocatalysts investigated here, ATR-IR spectra were collected as a function of time during the incubation samples at  $90^\circ\text{C}$ . Fig. 9 presents the evolution of the normalized signal at  $1620\text{ cm}^{-1}$  for RML, Lipozyme and RML/Chit at  $90^\circ\text{C}$ . The denaturalization reached a plateau for all materials after approximately 50 min. However, each material has a particular evolution in terms of denaturalization mechanism. On one hand, the unfold rate of pure RML is faster than in the commercial Lipozyme RM IM. Then, similar results were obtained when studying the evolution of the denaturalization of Lipozyme RM IM vs RML/Chit, which indicates that the thermal stability of our biocatalysts – from the IR point of view and its complexity – is close to the commercial one.

In the case of RML/Glut-Chit, it was not possible to identify significant differences in the spectra that could be attributed to conformational changes, because of the interference of the strong signals due to the reacted glutaraldehyde.

The deactivation of lipases by denaturalization is not considered as a simple process, from the native state to a final inactive form. On the contrary, this occurs through a series of intermediaries, which may have a lower or greater activity than the native state of the enzyme [21]. Noel and Combes [38] reported on the effect of temperature and pressure on the activity of RML using as a test reaction the esterification of lauryl acid with butanol. They found an irreversible loss of activity of 20% after 60 min incubation of the enzyme at  $50^\circ\text{C}$ , which decreases to 80% after 60 min at  $60^\circ\text{C}$ . The enzyme showed no activity after 10 min at  $70^\circ\text{C}$ . Additional

studies using fluorescence attributed the thermal inactivation of the enzyme aggregation processes rather than by conformational changes unfolding.

Our results on the denaturation of RML in biocatalysts are in agreement with those reported by Noel and Combes [38]. However, the analysis by IR-ATR of the amide I' region allows the discussion of more details about the secondary structure of the enzyme. In addition to aggregation, there are conformational changes with loss of  $\alpha$ -helix structure, which are inferred results in a loss of enzyme activity by thermal effect. Nevertheless, the overall thermal stability of RML was not significantly affected by the immobilization on chitosan.

### 3.4. Catalytic activity

Previous results have brought information about the amount, structure and thermal stability of RML immobilized on chitosan based supports. However, it is also necessary to check if the supported protein retained its catalytic activity after immobilization. To this end, the enzymatic activity of each biocatalyst was investigated using as a test reaction the hydrolysis of ethyl stearate at  $36^\circ\text{C}$ . The progress of the reaction was monitored by FTIR-ATR in situ as described in the experimental section.

Fig. 10A shows time-resolved infrared spectra in the  $\nu(\text{COO})$  region,  $1800\text{--}1600\text{ cm}^{-1}$ , collected during the hydrolysis of ethyl

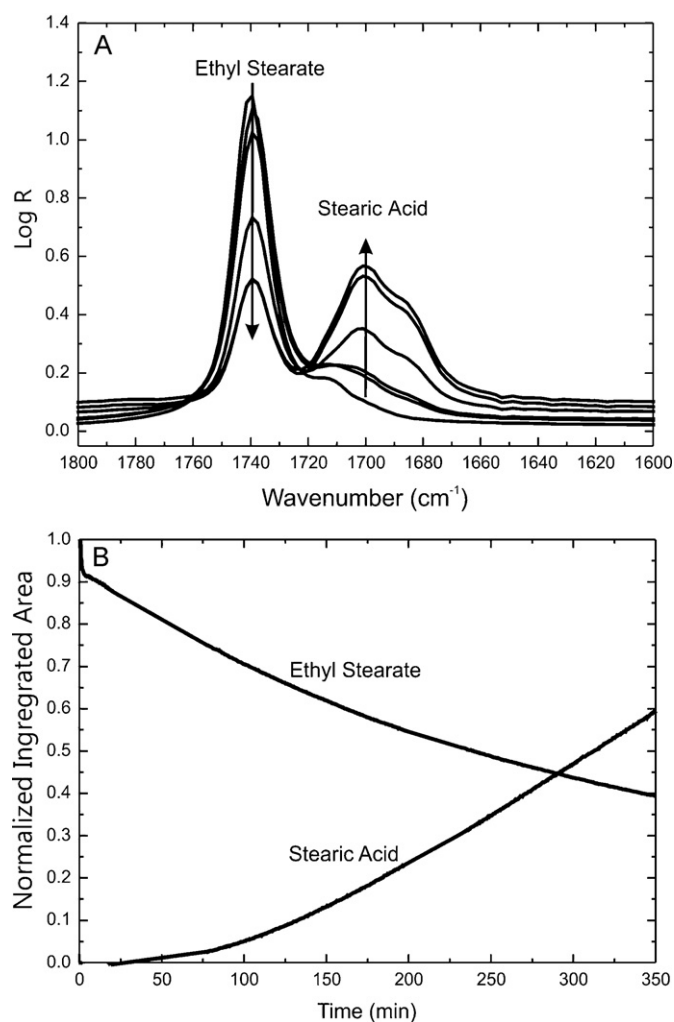


Fig. 10. ATR-FTIR spectra in the  $\nu(\text{COO})$  region during the hydrolysis of ethyl stearate to stearic acid using pure RML (A). Evolution of the integrated absorption of the ester and acid as a function of time (B).



**Table 4**  
Hydrolysis of ethyl stearate.

Biocatalyst	Conversion after 5 h (%)
RML gel <sup>a</sup>	53
Lipozyme	50
RML/Chit	57
RML/Glut–Chit	53
Chit	32
Glut–Chit	15

<sup>a</sup> No solid was obtained after vacuum treatment. No reaction was observed after 5 h in a blank experiment without solid.

stearate using pure RML catalyst. The hydrolysis of ethyl stearate results in the release of free fatty acids from the ester. The decrease of the carbonyl ester absorption frequency at  $1745\text{ cm}^{-1}$  allows monitoring the hydrolysis of the ester bond. Moreover, the carbonyl absorption frequency of free fatty acids (ca.  $1700\text{ cm}^{-1}$ ) is also suitable to follow the reaction in organic media [29,39]. As mentioned in the experimental section, in an additional experiment the proportionality between both IR signals of carbonyl in the ester and in the acid, and their concentration was verified. Fig. 10B present the evolution of the integrated absorption of the ester and acid as a function of time using free RML.

Approximately 53% conversion was reached after 5 h of reaction using pure RML. The test reaction was also investigated using Lipozyme RM IM, RML/Chit and RML/Glut–Chit and the bare supports, Chit and Glut–Chit. All the Chit supported biocatalysts presented a complication to follow the ethyl stearate hydrolysis due to adsorption of reactants and products on the Chitosan surface. Then, after 5 h of reaction, ATR-FTIR spectra were obtained after “washing” the sample with n-pentane into the ATR cell (200  $\mu\text{l}$  was aggregated with a micropipette). The characteristic signal of stearic acid at  $1700\text{ cm}^{-1}$  showed up. In turn, no lixiviation of the enzyme was observed during the reaction test in none of the biocatalysts tested. This finding correlates with the important loss of enzyme found in the washing solutions in the case of RML/Chit, leaving only strongly adsorbed RML on the Chit surface.

It must be emphasized here that the conversions results for the enzymatic catalyzed hydrolysis of ethyl stearate possess a *qualitative* character, with the main goal of corroborate the preservation catalytic activity after immobilization. When the method (ii), presented in Section 3.1 to quantify lipase, was applied as an additional approach, several confounders in the data were found. First, there may be diffusional problems for all the biocatalysts. Second, free RML is surely aggregated upon water evaporation from a solution and the results are not comparable to a reaction in a stirred vessel in an organic solvent. In this sense it is not a credible comparison term because the RML is not expressing its best enzymatic activity [34]. Third, commercial RML and Chit-supported RML have different supports in nature and in porosity therefore comparisons are not applicable. Fourth, no stirring of any kind was applied in the ATR cell, and therefore internal and external mass diffusion problems may be present. Nevertheless, this test is very useful as a fast measure of the efficiency of the immobilization process and the characterization of the activity in supported biocatalysts in comparison with free and commercial immobilized systems, considering the limitations of the test. It is also worth to mention, replications of these assays were performed and accurate results were obtained ( $\pm 5\%$  conversion).

Table 4 presents the conversion of ethyl stearate for each biocatalyst after 5 h of reaction. The immobilized RML samples show an ethyl stearate conversion in the range of 50–57%, while the Chit and Glut–Chit supports present a 30 and 15% conversion, respectively. The activity of the bare supports is related to the non-enzymatic reaction kinetics through the  $\text{NH}_2/\text{NH}_3^+$  surface sites in the chitosan. Moreover, as expected, the Glut–Chit solid showed a lower

activity, since several  $\text{NH}_2/\text{NH}_3^+$  groups are not available due to the anchoring of glutaraldehyde on these sites. When lipase reacts with Glut and/or adsorbs on the surface, the amino groups on the surfaces are even more blocked. The results allow us to speculate that the amount of *active* RML in Lipozyme and Chit supported biocatalysts are probably similar, beyond the determination of total PP. The results from Table 4 imply that the immobilization process does not alter significantly the original catalytic character of the enzyme, at least in the context of a test reaction like the one here studied.

#### 4. Conclusion

Biocatalysts from *Rhizomucor miehei* lipase immobilized onto chitosan-based supports were prepared by physical adsorption and covalent bonding to the support using glutaraldehyde. These biocatalysts were characterized by in situ FTIR-ATR spectroscopy and compared with pure RML and a commercial Lipozyme sample.

The amount of enzyme as precipitable protein was carefully determined on each catalyst. Several experimental problems arising during lipase quantification using UV/visible methods were addressed, suggesting that most of conventional methods do not provide an accurate protein quantification data regarding to the immobilization of RML in this kind of supports.

The infrared characterization of the supported RML showed that the enzyme was bounded to the Chit and the Glut–Chit with minor changes in its secondary structure, thermal stability and enzymatic activity in the selected reaction test.

#### Acknowledgments

This work was supported by the National Council for Scientific and Technical Research (CONICET), the National Agency for the Promotion of Science and Technology (ANPCyT, Grant PICT Red 729/06 and PME 311/062005).

#### References

- [1] X. Xu, *Funct. Foods Process. Inform.* 11 (2000) 1121–1130.
- [2] F.J. Contesini, P. de Oliveira Carvalho, *Tetrahedron: Asymmetry* 17 (2006) 2069–2073.
- [3] M.L. Foresti, M. Galle, M.L. Ferreira, L.E. Briand, *J. Chem. Tech. Biotech.* 84 (2009) 1461–1473.
- [4] V.M. Balcao, A.L. Paiva, F.X. Malcata, *Enzym. Microb. Technol.* 18 (1996) 392–416.
- [5] X.J. Huang, D. Ge, Z.K. Xu, *Eur. Polym. J.* 43 (2007) 3710–3718.
- [6] D.S. Rodrigues, A.A. Mendes, W.S. Adriano, L.R.B. Goncalves, R.L.C. Giordano, *J. Mol. Catal. B: Enzym.* 51 (2008) 100–109.
- [7] K.V. Harish Prashanth, R.N. Tharanathan, *Trends Food Sci. Technol.* 18 (2007) 117–131.
- [8] C.E. Orrego, N. Salgado, J.S. Valencia, G.I. Giraldo, O.H. Giraldo, C.A. Cardona, *Carbohydr. Polym.* 79 (2010) 9–16.
- [9] J. Brugnerotto, J. Lizardi, F.M. Goycoolea, W. Argüelles-Monál, J. Desbrieres, M. Rinaudo, *Polymer* 42 (2009) 3569–3580.
- [10] A. Dincer, A. Telefoncu, *J. Mol. Catal. B: Enzym.* 45 (2007) 10–14.
- [11] M.L. Foresti, Tesis Doctoral en Ingeniería Química, Universidad Nacional del Sur, 2006.
- [12] S. Servagent-Noinville, M. Revault, H. Quiquampoix, M.H. Baron, *J. Colloid Interface Sci.* 221 (2000) 273–283.
- [13] J.M. Palomo, R.L. Segura, G. Fernández Lorente, R. Fernández Lafuente, *J.M. Guisán, Enzym. Microb. Technol.* 40 (2007) 704–707.
- [14] K. Matsuo, R. Yonehara, K. Gekko, *J. Biochem.* 135 (2004) 405–411.
- [15] Barth, *Biochim. Biophys. Acta* 1767 (2007) 1073–1101.
- [16] H. Fabian, W. Mantele, *Infrared spectroscopy of proteins*, in: J.M. Chalmers, P.R. Griffiths (Eds.), *Handbook of Vibrational Spectroscopy*, John Wiley & Sons, Inc., Chichester, 2002, pp. 3749–3775.
- [17] J. Kong, S. Yu, *Acta Biochim. Biophys. Sin.* 39 (8) (2007) 549–559.
- [18] V. Lassalle, S. Pirillo, E. Rueda, M.L. Ferreira, *Proc. XXI Congreso Iberoamericano de Catálisis*, 2010, AP-9, p. 106.
- [19] R.B. Hernández, A.P. Franco, O.R. Yola, A. López-Delgado, J. Felcman, M.A.L. Recio, A.L. Ramalho Merce, *J. Mol. Struct.* 877 (2008) 89–99.
- [20] S. Noinville, M. Revault, M. Baron, A. Tiss, S. Yapoudjian, M. Ivanova, R. Verger, *Biophys. J.* 82 (2002) 2709–2719.
- [21] P.I. Haris, F. Severcan, *J. Mol. Catal. B: Enzym.* 7 (1999) 207–221.



- [22] Z.S. Derewenda, U. Derewenda, G.G. Dodson, J. Mol. Biol. 227 (1992) 818–839.
- [23] E. Goormaghtigh, J.-M. Ruysschaert, V. Raussens, Biophys. J. 90 (2006) 2946–2957.
- [24] E. Goormaghtigh, R. Gasper, A. Bénard, A. Goldsztein, V. Raussens, Biochim. Biophys. Acta 1794 (2009) 1332–1343.
- [25] B. Altavara, M.I. Burguete, E. García-Verdugo, S.V. Luis, M.J. Vicent, Tetrahedron 57 (2001) 8675–8683.
- [26] M. Petkar, A. Lali, P. Caimi, M. Daminati, J. Mol. Catal. B: Enzym. 39 (2006) 83–90.
- [27] J. Brugnerotto, J. Lizardib, F.M. Goycooleab, W. Arguelles-Monalc, J. DesbrieAresa, M. Rinaudo, Polymer 42 (2001) 3569–3580.
- [28] O.A.C. Monteiro, C. Airoidi, Int. J. Biol. Macromol. 26 (1999) 119–128.
- [29] L.J. Bellamy, The Infrared Spectra of Complex Molecules, third ed., Chapman & Hall, London, 1975.
- [30] J.M. Palomo, G. Fernández Lorente, C. Mateo, C. Ortiz, R.F. Lafuente, J.M. Guisán, Enz. Microb. Technol. 31 (2002) 775.
- [31] M.L. Ferreira, M.E. Gschaidler, Macromol. Biosci. 1 (2001) 233–248.
- [32] H.S. Mansur, R.L. Orefice, A.A.P. Mansur, Polymer 45 (2004) 7193–7202.
- [33] I. Migneault, C. Dartiguenave, M.J. Bertrand, K.C. Waldron, BioTechniques 37 (2004) 790–802.
- [34] D.R. Walt, V.I. Agayn, Trends Anal. Chem. 13 (1994) 425–430.
- [35] S. Margel, A. Rembaum, Macromolecules 13 (1980) 19–24.
- [36] K. Hashihoto, Y. Masada, Y. Sumida, T. Tashi, N. Satoh, Int. J. Mass Spectrom. Ion Phys. 48 (1983) 125–129.
- [37] A.M. Brzozowski, Z.S. Derewenda, E.J. Dodson, G.G. Dodson, J.P. Turkenburg, Acta Crystallogr., Sect. B 48 (1992) 307–319.
- [38] M. Noel, D. Combes, J. Biotechnol. 102 (2003) 23–32.
- [39] T. Snabe, S.B. Metersen, J. Biotechnol. 95 (2002) 145–155.